Mathematical Modelling, Design, and Optimization of Electrochemical Capacitors from Layered Materials

INNOCENT S. IKE [a,b,c], Iakovos Sigalas [a,b], Sunny Iyuke [a] and Kenneth I. Ozoemena [d,e]

[a] School of Chemical & Metallurgical Engineering and DST-NRF Centre of Excellence in Strong Materials, University of the Witwatersrand, Johannesburg, South Africa

[b] Materials for Energy Research Group (MERG), University of the Witwatersrand, Johannesburg, South Africa

[c] Department of Chemical Engineering, Federal University of Technology Owerri Nigeria,

[d] CSIR Materials Science and Manufacturing, Pretoria, South Africa

and [e] School of Chemistry, University of the Witwatersrand, Johannesburg, South Africa

The image cannot be displayed. Your computer may not have enough memory to open the image, or the image may have been corrupted. Restart your computer, and then open the file again. If the red x still appears, you may have to delete the image and then insert it again.

INTRODUCTION

Electrochemical Capacitors (Ecs) are electrical energy storage devices that store charges through either electrostatic charging of a double layer or through a Faradaic reaction or through both mechanisms. It has higher energy density than conventional electrostatic capacitors and as well higher power density than batteries in general.The key performance parameters of electrochemical capacitors are specific capacitance, energy density, power density, rate capability and cycling stability [3].

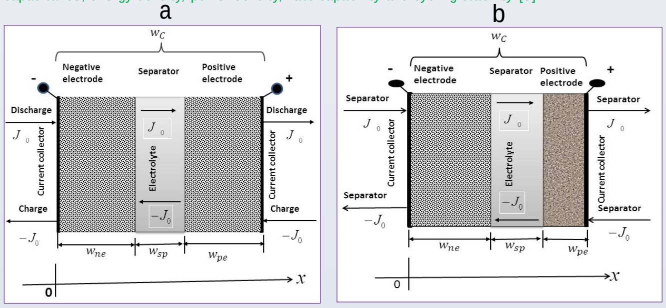

Figure 1. (a) symmetric electrochemical capacitor cell, (b) asymmetric electrochemical capacitor cell showing various functional layers on the macroscale [1].

AIMS AND OBJECTIVES

The aims of this study is to develop mathematical models for various of ECs and build theoretical basis to examine the effects of self-discharge, operating conditions and design configurations on the Performance of the devices. To also optimize the ECs design parameters and operating conditions for high energy and power performances . Also to develop a realistic guideline for design optimal design of ECs enhanced performance parameters like specific energy, power density, lifecycle and energy retention

THE MATHEMATICAL MODELS

$$\frac{\partial \varphi_{ne}(x,t)}{\partial t} = \beta^2 \frac{\partial^2 \varphi_{ne}(x,t)}{\partial x^2} + \frac{J_{VR}(x,t)}{C_V} \qquad 1$$

$$\beta^2 = \frac{\alpha_1 \alpha_2}{C_V(\alpha_2 + \alpha_1)} \qquad 2$$

$$J_{VR}(x,t) = J_{VR1}(x,t) = J_{VR2}(x,t) \qquad 3$$

$$\rho C_p \frac{\partial T_{(x,y,z,t)}}{\partial t} = \nabla\left(\lambda_{(x,y,z,t)} \nabla T_{(x,y,z,t)}\right) + Q_{G(x,y,z,t)} \qquad 4$$

RESULTS AND DISCUSSIONS

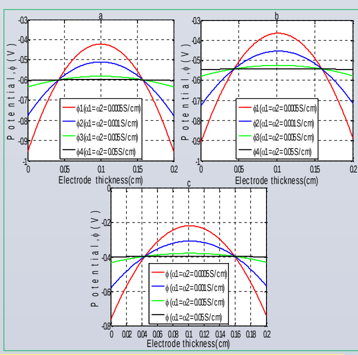

Figure 2: Electrode potential profiles as a function of position after after charge process for(a) EC without self-discharge (b) EC with self-discharge due to only EDLs instability, and (c) EC with self-discharge due to both side-reactions/redox reactions and EDLs instability.

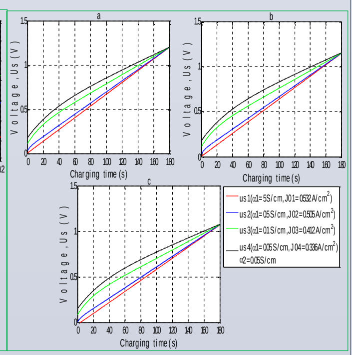

Figure 3: EC voltage dependence on time during charge process from 0V to 1.2V for (a) EC without self-discharge (b) EC with self-discharge due to only EDLs instability, and (c) EC with self-discharge due to both side-reactions/redox reactions and EDLs instability.

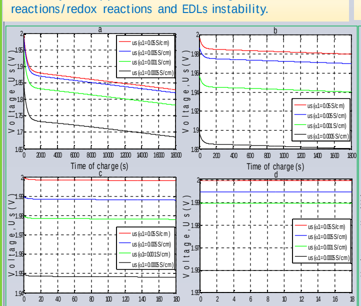

Figure 4: The voltage decay of asymmetric ECs of various electrodes effective conductivity over time by self-discharge due to both side-reactions/redox reactions and EDLs instability for charge process from 0.8V to 2.0V (a) 18000s charging,(b) 1800s charging, (c) 180s charging and (d) 18s charging.

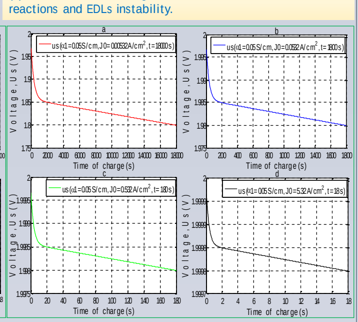

Figure 5: The voltage decay of asymmetric ECs over time by self-discharge due to both side-reactions/redox reactions and EDLs instability for charge process from 0.8V to 2.0V (a) 18000s charging,(b) 1800s charging, (c) 180s charging and (d) 18s charging.

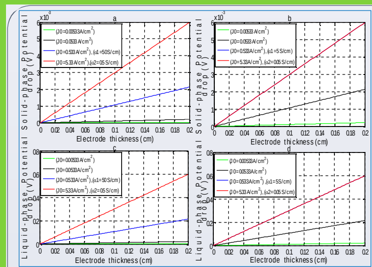

Figure 6. Solid-phase potential drop for ECs charged at various current densities and of electrode and electrolyte effective conductivity (α1 & α2) of (a)50S/cm & 0.5S/cm, (b) 5S/cm & 0.05S/cm; liquid-phase potential drop for ECs charged at various current densities and of α1 and α2 of (c)50S/cm & 0.5S/cm, (d) 5S/cm & 0.005S/cm;

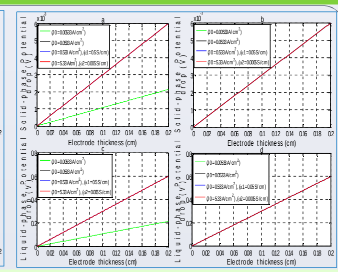

Figure 7. Solid-phase potential drop for ECs charged at various current densities and of effective conductivity (α1 & α2) of (a)0.5S/cm & 0.005S/cm, (b) 0.05S/cm & 0.0005 S/cm; liquid-phase potential drop for ECs charged at various current densities and of α1 and α2 of (c)0.5S/cm & 0.005S/cm, (d) 0.05S/cm & 0.0005S/cm;

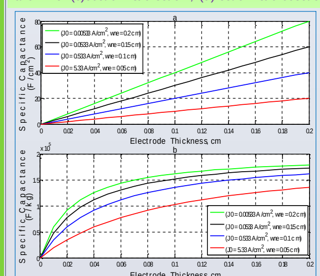

Figure 8. Specified capacitance for various electrode widths at various current densities (a) per square centimetre (cm^2), and (b) per kilogram of the ECs.

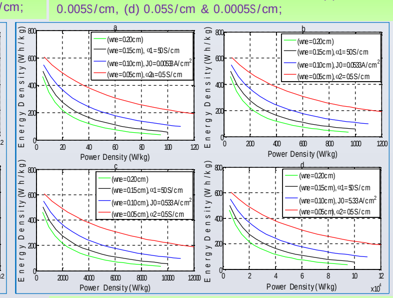

Figure 9. Ragone plots of ECs with various effective conductivities α1=50S/cm, α2 =0.5S/cm charged at (a) 0.00533A/cm^2 for 18000s, (b) 0.0533A/cm^2 for 1800s, (c) 0.533A/cm^2 for 180s, and (d) 5.33A/cm^2 for 18s.

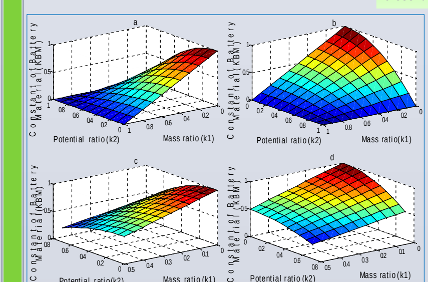

Figure 10. Profile of the value of K_{BM} as a function of the mass and operating potential window ratio factors of the battery-kind electrode for 3-D side view of (a) side of 0 < k1 ≤ 1 and 0 < k2 ≤1 limits and ; (b) front of 0 < k1 ≤ 1 and 0 < k 2 ≤ 1 limits and ;(c) side of 0 < k1 ≤ 0.5 and 0 < k2 ≤ 0.7 limits ; and (d) front of 0 < k1 ≤ 0.5 and 0 < k2 ≤ 0.7 limits

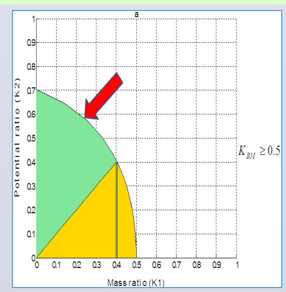

Figure 11. Profile of conditions of k1 and k2 for higher values of both energy and power density of asymmetric ECs ED_{as} and PD_{as} in comparison with the values of energy and power density of symmetric ECs ED_s and PD_s.

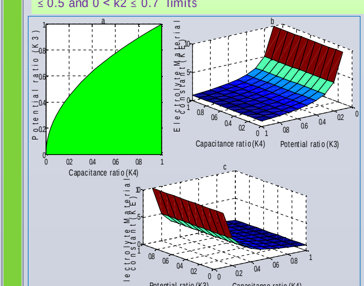

Figure 12. (a) Profile of the given condition of $K_E \geq 1.0$ as a function of k_3 and k_4 ratios; (b) front view of the value of electrolyte material-associated constant K_E as a function of k_3 and k_4 ratios; and (c) side view of the value of K_E as a function of k_3 and k_4 ratios.

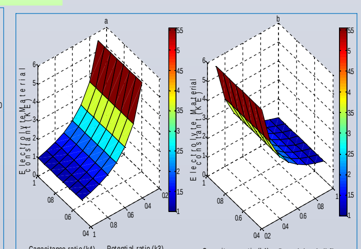

Figure 13. (a) Profile of the value of K_E as a function of k_3 and k_4 ratios for ranges of $0.3 \leq k_3 < 1$ and $0.5 \leq k_4 < 1$; and (b) 3-D side view profile of the value of electrolyte material-related constant K_E as a function of k_3 and $k_4$ratios for ranges of $0.3 \leq k_3 < 1$ and $0.5 \leq k_4 < 1$.

CONCLUSIONS

ECs with self-discharge loss some of the storable energy as self-discharge during the device charging and discharging processes. Charging and discharging the device fast reduced the rate of the self-discharge. The amount of current density that should be employed to successfully charge ECs is greatly dependent on the effective conductivities of the electrode and electrolyte as well as electrodes thickness. Therefore, ECs of low electrode and electrolyte effective conductivities cannot be charged effectively at high current density, because potential drops in the liquid-phase will be as high as half the cell's voltage. The typical length scale [w_e] over which liquid potential drop occurs can be employed as design parameter to optimize electrodes thickness for ECs designed to function under a given current density spans. Ragone plots of ECs with diverse electrode thicknesses and different effective conductivities α1 and α2 charged at different current densities can be utilized to select electrode dimensions to attain a given energy and power density specifications . Asymmetric EC with suitable electrode mass and operating potential range ratios has over two-fold E_{ch}, E_{dis}, ED_{max} and PD_{max} higher than those of symmetric EDLC using the same aqueous electrolyte. Also, asymmetric EC proper electrode mass and operating potential range ratios joined with appropriate organic electrolyte has over five-fold E_{ch}, E_{dis}, ED_{max} and PD_{max} higher than those of similar asymmetric EC using aqueous electrolyte. These results can be a great guideline for design, fabrication and operation of EC of outstanding performance in terms of high energy and power densities.